Factorial Tests on Process Operating Conditions and Bed Fines on the Circulating Fluid Bed Performance

Lawrence J. Shadle,*,† James Spenik,‡ Angela Sarra,† and John Ontko†

National Energy Technology Laboratory, U.S. Department of Energy, 3610 Collins Ferry Road, Morgantown, West Virginia 26507-0880, and REM Engineering Services PLLC, 3537 Collins Ferry Road, Morgantown, West Virginia 26505

A cold-flow circulating fluid bed (CFB) was operated using coke breeze with a packed-bed standpipe over a range of riser and standpipe air flows. The bed materials were selected to simulate solids flow in a CFB gasifier (carbonizer) but are generally relevant to most CFB processes. CFB tests were conducted primarily in the transport mode with sufficient gas velocity to achieve a uniform axial riser pressure profiles over most of the riser height. The independent variables tested included the riser gas velocity, aeration at the base of the standpipe, and concentration of fines (average particle size). The solids inventory and riser outlet pressure were maintained constant. Factorial tests were conducted in randomized order and in duplicate to provide and an unbiased estimate of the error. Fines were tested as a blocked variable. The gas velocity, standpipe aeration, and relative amount of fine particles were all found to be significant factors affecting both the riser solids holdup and solids flux. The riser pressure drop and mass circulation increased at the higher level of fines contrary to some earlier reports in the literature. The riser pressure drop was fitted using the general linear model (GLM), which explained more than 98% of the variation within the data, while a GLM for the mass circulation rate explained over 90%. The uncertainty of process operating variables was characterized independently through a series of duplicated flow proving experiments.

Introduction

Circulating fluid bed (CFB) reactors have found increasing applications in fluid bed catalytic crackers and coal combustion, and now this technology is being applied to coal carbonization,[1,2] gasification,[3,4] and hot gas cleanup.[5,6] While CFB combustion has developed in the fast fluidized bed (FFB) regime to take advantage of the high mass and heat transfer in the dense bed regions of the reactor, gasification reactions are endothermic and thus have less stringent heat-transfer requirements and will benefit from smaller pressurized reactors with higher coal throughput. As a result, there is interest in operating at higher velocities yet maintaining gas−solids mixing via high solids recycle rates. This puts a significant burden on the solids separation devices, not to mention materials of construction, to minimize erosion. There is a need to understand the effects on the performance of CFB reactors operating at higher gas velocities, higher solids recycle, and higher fines concentrations.

Research has demonstrated that the particle size distribution (PSD) has an important impact on many hydrodynamic properties including the minimum fluidization velocity and elutriation rate.[7−14] Gauthier et al.[7] found that a narrow PSD reduces defluidization and segregation. Flat distributions and bimodal distributions tend to segregate upon defluidization. Gaussian distributions also have lower U_{mf} than narrow distributions.[8] Cheung et al.[10] proposed that smaller particles fill the void spaces between the larger particles, lubricating the coarse particles, reducing friction, and thus lowering the minimum fluidization velocity. Geldart and co-workers[11,12] reported that fines aid in the elutriation of coarse particles from a fluidized bed. Kwauk[13] identified that the momentum of the fines aided the elutriation of particles, and Choi et al.[14] found that the elutriation rate of large particles increases nearly proportionally to the increase in the upward momentum of the fines on a mass fraction basis. The effect of fines on elutriation of coarse particles decreases as the gas velocity increases. The elutriation rate of fines, however, is relatively insensitive to the PSD.

Several researchers recently found that both the particle size and PSD also influence the gas−solid transport processes.[15,16] Hyder et al.[15] studied the effect of the mean particle size on lean transport along horizontal lengths, finding that the apparent solids holdup or ΔP increases for larger particles. This effect is greatest for smaller particles and lower gas velocities. Hayden et al.[16] characterized the gas velocity required to pick up different particles and found that for very small particles (10 μm) the packing density and pickup velocity are constant. Particle−particle interactions and electrostatic forces dominate for particles between 10 and 50 μm, resulting in lower pickup velocities needed for larger particles in this size range. Above this particle size, inertial forces dominate and higher velocities are required for larger particles.

The CFB fluidization regime was first thought to depend only upon the gas velocity and solids flux.[17,18] Later studies demonstrate that the system geometry (i.e., entrance and exit effects, diameter, and height),[19−23] operating pressure,[24] and particle properties[24−29] also affect the gas−solid hydrodynamics and axial solids distributions. Several researchers evaluated the effect of the particle size on the riser in the FFB regime.[26−28]

* To whom correspondence should be addressed. Tel.: (304) 285-4647. E-mail: lshadl@netl.doe.gov.

† U.S. Department of Energy.

‡ REM Engineering Services PLLC.

Sun and Grace[26] reported that the ozone conversion efficiency, indicative of gas−solids mixing, is generally higher for wide PSD in the turbulent and FFB regimes, though little particle size effect is observed for low velocities.

Bai et al.[27] found that in the FFB regime the solids profile has lower solids fractions at the bottom of the riser when using smaller particles. This difference becomes less pronounced as the gas flow increases and/or as the solids flux decreases. Adanez et al.[28] demonstrated that both smaller particles and less dense solids produce lower solids holdup, decreasing the solids fraction in the riser, at a given gas velocity and circulation rate. However, contrary to these research findings, when the fines content increases in practice as a result of improvement of the cyclone solids separator efficiency, a quite different effect is observed.[29] Lee found that the overall solids holdup increases with more fines, contrary to the laboratory tests. In particular, the upper dilute region increases in solids loading and dominates the overall riser response, even though the lower dense region did exhibit the expected lower solids fraction. One purpose of these experiments is to better understand these apparent disparate results.

One clue to this apparent contradiction is found by considering the response of the recycle leg of a CFB to variations in particle properties.[30−32] Kim and Kim[30] evaluated the effect of the particle size and density on the performance of the recycle leg, i.e., standpipe and loopseal. The rate of solids flux attained per unit volumetric aeration increased as the particle size decreased; however, the fluidization number (U_{move}/U_{mf}) was lower with larger particles. Smaller particles fill the void and drag relatively more gas down the standpipe with the solids,[31] requiring a higher fluidization number to achieve comparable ΔP buildup in the standpipe.[32] Kim and Kim found that smaller particles produce less ΔP in the weir section of the loopseal but a higher ΔP in the riser and standpipe for a given circulation or aeration rate.

Also, within these available studies, there are no reports of duplicate tests, and thus there are little data available to estimate the experimental error and the uncertainty of operating variables. Much of the reported data lack specification of some important parameters. For instance, the actual location for the experimental pressure is seldom reported. Likewise, the values of the ambient temperature, the fines concentration, and the solids inventory are often omitted from the experimental description. These secondary parameters can influence the repeatability if the barometric pressure, ambient temperature, solids shape, or fines concentration changes from test to test. A test referenced to 1 bar of pressure at the top of the riser can have 15% lower flow velocity than one referenced to 1 bar of pressure at the base of the riser when a dense bed material is used at a relatively high solids holdup in a relatively tall riser. As a result, the method of comparing test data with computer simulations is limited to qualitative and anecdotal evidence.

The results in this study are presented not as the most accurate CFB data set but rather as data rigorously characterized and qualified in terms of their uncertainty using statistically designed experiments. The premise undertaken was that the riser would be operated above the transport velocity defined by Yerushalmi and Cankurt[18] and beyond the physical configuration constraints as identified by Smolders and Baeyens.[33]

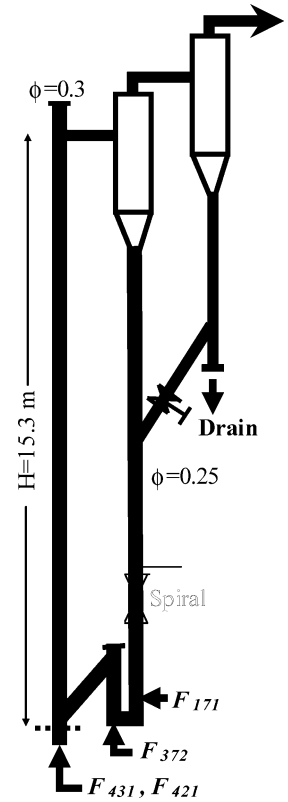

Figure 1. Schematic of the CFB test unit indicating a gas−solids separation system, aeration, and Spiral locations. Flow variables, F_i, are given in Table 3.

Experimental Description

A schematic of the cold-flow CFB model is presented in Figure 1. The riser is constructed of flanged steel sections, with three 1.22-m acrylic sections installed 2.4, 6.0, and 9.0 m above the solids feed location. The solids enter the riser from a side port of 0.23 m in diameter and 0.27 m above the gas distributor. Solids exit the riser through a 0.20-m port at 90° about 1.2 m below the top of the riser at a point 15.45 m above the solids entry location (centerline to centerline). Riser velocities were corrected for temperature and pressure as measured at the outlet of the riser. The air's relative humidity was maintained between 40 and 60% to minimize the effects of static charge building up on the solids. Flows utilized did not produce any significant pressure drop due to gas flow. Twenty incremental differential pressures were measured across the length of the riser using transmitters calibrated within 0.1% of full scale or about 2 Pa/m. The primary response measurement was the overall riser pressure differential, and it was calibrated within 0.45 Pa/m. Mass circulation rates were continuously recorded by measuring the rotational speed of a twisted spiral vane located in the packed region of the standpipe bed.[34] This calibrated volumetric measurement was converted to a mass flux using the measured packed-bed density presented in Table 1 and assuming that the packed-bed void fraction at the point of measurement is constant (i.e., $\epsilon_b = 0.45$). Analysis of the standpipe pressure profile, estimated relative to gas−solids velocities, and bed heights has

Table 1. Bed Material Properties

characteristics	initial coke bed material	dipleg coke fine	coke bed + 20% fines
size distribution			
d_p (μm)	258	89	211
σ_p (μm)	10.0	6.6	11.6
d_c (μm)	458	199	444
n	2.68	1.73	2.18
particle density			
ρ_s (kg/m^3)	1503		
packed bed			
ρ_{bulk} (kg/m^3)	885	948	923
ϵ_{packed}	0.41	0.37	0.39
fluidization properties			
U_{mf} (cm/s)	3.2	2.3	
ϵ_{mf}	0.48		
U_t (cm/s)	20		

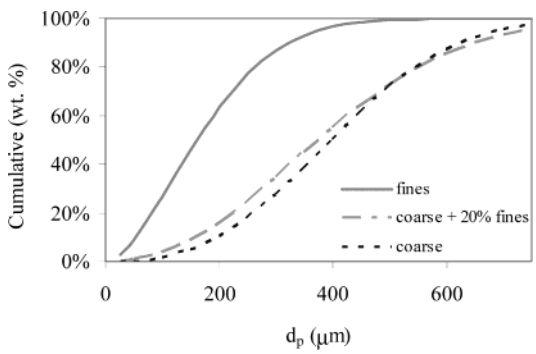

Figure 2. Average size distribution of coarse coke bed material, coke fines collected from dipleg below the secondary cyclone, and a 20% mixture of fines with the coarse coke bed material.

indicated that this constant voidage estimate is reasonable over the range of operating conditions reported here.

The size distribution for the coke material was characterized using a standard wire-mesh sieve analysis. The fines used for these tests were separated aerodynamically in situ during the CFB process over a period of over nearly 100 h of operation. It was identified that the coke material was, in fact, breaking down at higher gas velocities; therefore, solids collected in the dipleg below the secondary cyclone were separated from the recycle stream. This was accomplished by closing a valve, isolating the dipleg from the standpipe, and then draining the dipleg periodically from the dipleg. These dipleg solids were combined, sampled, and analyzed (Figure 2). The size distribution was calculated using a Sauter mean particle size for the fines of 89 μm. The distribution or spread was estimated by calculating the standard deviation from the mean, σ_s. Rosin−Rammler parameters were determined from the sieve analysis using the following equation:

$$Y = 1 - e^{-(d/d_c)^n} \tag{1}$$

where d is the sieve size, Y is the cumulative weight percent, d_c is the characteristic diameter, and n is the characteristic size distribution or spread. The Rosin−Rammler fit to these cumulative distributions is shown in Figure 2, and the parameters of the distributions are listed in Table 1. Each distribution is weighted within itself. The coarse distribution had fewer fines, whereas the larger particles within the mixture made up a smaller fraction of the distribution. As a result, the coarse distribution curve intersected the line representing the mixture.

Table 2. Coefficients for Coded Value Transformation Using Equation 1

independent param	α	β
U_g (m/s)	6.10	0.76
U_{move} (cm/s)	3.87	0.85
Fines (%)	10	10

The particle density was measured using water displacement, taking care to wet the surface completely. The coke surface is sufficiently hydrophobic to avoid filling any porosity with water. The minimum fluidization velocity was measured in a 5-cm-diameter cylindrical bed using the increasing gas velocity method. The sphericity was estimated by fitting the Ergun equation to the pressure drop versus velocity profile taken prior to fluidization. The terminal velocity was calculated from drag laws using the measured solids density average particle size and sphericity.

Test operating conditions were varied by adjusting the riser flow or the aeration at the base of the standpipe while maintaining a constant system outlet pressure at 0 kPa using a back-pressure control valve. Steady-state conditions were defined as holding a constant set of flow conditions and maintaining a constant response in the pressure differentials over a 5-min period. All steady-state test results represent an average over that 5-min period.

The independent variables tested included the riser gas velocity, U_g, the aeration near the base of the standpipe, U_{move}, and the concentration of *fines* or particle size. The solids inventory and riser outlet pressure were maintained constant. The solids were recycled from the primary cyclone only. *Fines* were tested as a blocked variable. The first sets of tests were conducted on coarse bed material. Then dipleg fines were added gradually to the top of the standpipe, taking care to blend it with the coarse inventory; the CFB was operated for 8 h to continue mixing; and finally solids were removed from the base of the standpipe to restore the total amount of solids in the CFB loop back to the initial inventory. The operating conditions were then established to repeat the factorial test conditions with bed material including the dipleg *fines*. Tests were set up using coded variables with a high level (+1) and a low level (−1). The actual levels with appropriate engineering units for the independent parameters, X, are obtained by transforming the data using eq 2 and Table 2 identifying the coefficients

$$X = \alpha + \beta I \tag{2}$$

where α and β are the average and differential coefficients and I is the coded level.

The primary response variables were the pressure drop across the entire length of the riser, ΔP_r, the solids flux, G_s, and the standpipe bed height, H_{sp}. The apparent riser voidage profile was obtained from each of the incremental ΔP measurements taken along the riser height using the following relationship:

$$\Delta P/\Delta L = \rho_s(1 - \epsilon)g_c \tag{3}$$

$$\epsilon = 1 - \Delta P/\Delta L \rho_s g_c \tag{4}$$

where ϵ is the apparent voidage in the increment ΔL, assuming that ΔP is equal to the weight of the solids, ρ_s is the solids density, and g_c is the gravitational constant.

Table 3. Relative Contribution of Various Instruments to the Total Expected Error in U_g Calculation

variable	units	value	derivative	Δu_n	$(\Delta u_n \times \text{derivative})^2$	% contribution
F_{431}	m^3/h	2124.0	0.0036	85.36	9.38×10^{-2}	99.828
F_{421}	m^3/h	0	0.0000	28.45	0.00	0.000
F_{372}	m^3/h	25.488	0.0036	0.48	3.02×10^{-6}	0.003
T_r	C	18.33	0.0097	1.11	1.16×10^{-4}	0.123
$P_{r,base}$	kPa	0.08	0.0007	8.43	3.70×10^{-5}	0.039
P_{atmos}	kPa	0.99	−0.0007	3.25	5.51×10^{-6}	0.006
sum					9.40×10^{-2}	100.000

Measurement Uncertainty in CFB Quantities

Several important factors in the design and operation of a CFB are calculated values based on various individual measured quantities, each of which has an inherent inaccuracy. Given the individual inaccuracy of each measurement that goes into a calculation, the overall inaccuracy of the calculated value can be determined through the propagation of errors.[35] An attempt was made to understand the uncertainty in several important CFB quantities. These quantities include the riser superficial gas velocity, gas density, system inventory, solids flux, Reynolds number, and other calculated values. Here we consider the uncertainty for the superficial gas velocity, U_g, in detail and to a lesser extent that of U_{move} and riser ΔP. The uncertainty in the solids flux is considered in detail in reports describing in situ measurement and calibration methods for the Spiral instrument.[34,36]

The superficial gas velocity, U_g, is an important parameter in the characterization of CFB operation. Therefore, an understanding of the errors associated with the calculation of this parameter is important. The superficial gas velocity, in our case, was calculated using the conservation of mass and the ideal gas law as shown in eq 5.

$$U_g = \frac{V}{A_r}\frac{P_{std}}{P_{act}}\frac{T_{act}}{T_{std}} \tag{5}$$

Instrumentation was used to determine the mass flow rate of the gas, total static pressure, and system temperature. The flow area, A_r, was known from the geometry of the system. The system pressure was regulated by a valve located at the exit of the secondary cyclone. Because of the wide range of superficial gas velocities investigated, mass flows were controlled by two separate controllers. Although the controllers are commonly called "mass flow controllers", the actual control variable was based upon the volumetric flow for air at standard conditions (24 °C at 1.01 kPa). One controller, designated as F_{431}, has a larger range (0−4248 m^3/h) and was used during higher mass flow situations. F_{421}, a smaller range controller (0−1416 m^3/h), was used in lower flow situations. A third controller, F_{372} (0−113 m^3/h), was used to fluidize the loopseal, but its flow contributed to that in the riser (see Figure 1). The operation temperature, T_{act}, was determined by a thermocouple inserted near the distributor plate. The operating pressure, P_{act}, was the sum of the atmospheric pressure as determined using a barometer, P_{atmos}, and the pressure differential between the riser and atmosphere $P_{r,base}$. Substituting instrumentation nomenclature into eq 5 results in eq 6. Uncertainties in the

$$U_g = \left(\frac{F_{431} + F_{421} + F_{372}}{3600A_r}\right)\left(\frac{P_{std}}{P_{atmos} + P_{r,base}}\right)\left(\frac{T_r}{T_{std}}\right) \tag{6}$$

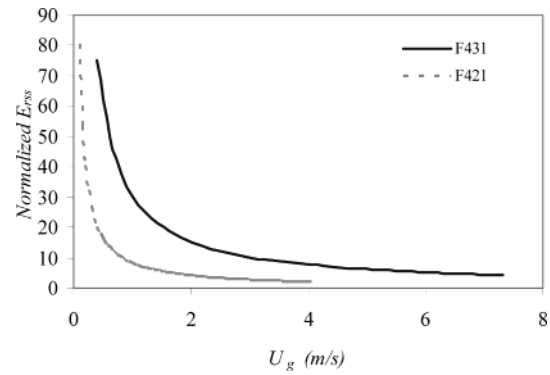

Figure 3. Probable error (root mean square) in mass flow rates as a function of the flow.

parameters V, A_r, P_{act}, and T_{act} will cause deviations in the value of U_g. A common method of determining the error propagated through a series of measurements is use of the root-sum-square formula,[35] as illustrated in eq 7. Uncertainties in individual measurements are

$$E_{rss} = \sqrt{\left(\Delta u_1 \frac{\partial f}{\partial u_1}\right)^2 + \left(\Delta u_2 \frac{\partial f}{\partial u_2}\right)^2 + \ldots + \left(\Delta u_i \frac{\partial f}{\partial u_i}\right)^2} \tag{7}$$

designated by Δu_i and may be considered as absolute limits on the errors, as statistical bounds such as 3σ limits or other modes of expressing uncertainty. However, they must be consistently applied throughout the equation. The function, f, is the equation for the desired variable (eq 6), and u_i values are the components of the variable.

Table 3 lists the relevant components of eq 6. Errors were assumed to be constant throughout the range of each instrument and were given as a function of the overall range of the instrument. Usually when controller F_{431} was employed, F_{421} was not and visa versa; otherwise, the error is the sum of both flow controllers.

Figure 3 was created using eq 7 and incorporating the values of Table 3. The absolute values, normalized to a percentage of full scale, of the expected uncertainty of U_g are portrayed in Figure 3 for a range of flow inputs, F_{431} and F_{421}, while the remaining three variables were held constant: $F_{372} = 42$ Nm^3/h, $P_{r,base} = 8.3$ kPa, and $T_r = 18.3$ °C. Clearly, the uncertainty in U_g was most pronounced when operating in the lower range of controllers F_{431} and F_{421}. Greater uncertainty while operating in the lower ranges is due to the error being evaluated as a function of full scale. Evaluation of the error based on full scale is an acceptable method because it accounts for both bias and random error. This demonstrates the need for diligence in selecting the proper instrument for expected conditions. Instruments should be nominally operated in the region of approximately 70% of full scale.

Examination of the components of the radicand in eq 5 can show the relative contribution to this overall error

Table 4. Particle Size Analysis of Grab Samples (Average of Three) Taken during Factorial Tests

		independent param			dependent param			
		coded			Rosin−Rammler		Sauter mean,	avg ρ_{bulk}
std no.	test ID	Fines	F_m	U_g	n	d_c (μm)	d_p (μm)	(kg/m^3)
1	f2	−1	−1	−1	2.64	454	253	880
9	f6	−1	−1	−1	2.66	461	258	880
5	f1	−1	−1	1	2.50	444	242	900
13	f3	−1	−1	1	2.64	452	253	890
11	f5	−1	1	−1	2.67	455	257	890
3	f4	−1	1	−1	2.70	462	261	900
15	f8	−1	1	1	2.87	475	274	880
7	f7	−1	1	1	2.75	463	262	870
2	f26	1	−1	−1	2.22	444	213	950
10	f18	1	−1	−1	2.06	430	197	930
14	f24	1	−1	1	2.30	453	221	930
6	f21	1	−1	1	2.11	438	206	910
4	f22	1	1	−1	2.18	443	212	930
12	f23	1	1	−1	2.38	464	230	920
8	f25	1	1	1	2.18	447	214	920
16	f20	1	1	1	2.18	445	212	910

contribution for each component. For F_{431} flow at the midrange rate of 2124 Nm^3/h, with no flow from F_{431}, and the other factors the same as listed in Table 3, it can be seen that the largest contributor to the overall error is the main flow controller, while the other instrument errors are minor.

The uncertainty in move aeration is determined by the same method as that of the superficial gas velocity. Therefore, the largest contributor to the uncertainty was found to be the flow controller F_{171} with a maximum flow rate of 28.3 Nm^3/h. Calculating the error based on 2% of full scale, the uncertainty of the true values of the independent parameter U_{move} is approximately 0.3 cm/s. The uncertainty in ΔP_r was found to be approximately 0.08 kPa based on 0.04% of full-scale error.

Results and Discussion

Tests were developed to simulate solids flow in a coal-fired CFB gasifier or carbonizer but are generally relevant to CFB conversion of coal and associated process solids. A coal-derived bed material was selected to provide an accurate representation of the shape and density of coal-derived products. Coke breeze was chosen because it is a relatively hard material resistant to attrition and can be obtained in appropriate sizes for CFBs and in commercial quantities for large-scale fluidization testing. The size distribution is presented in Figure 2, and the primary physical and fluidization characteristics can be found in Table 1. The starting coke bed material had a relatively broad size distribution with a Sauter mean diameter, d_p, of approximately 258 μm. After adding fines, d_p dropped to about 211 μm. The distribution was only slightly broader with added fines, with a measured standard deviation of 11.6 μm compared to 10 μm for the initial bed material. Characterizing the particle size using the Rosin−Rammler distribution indicated that the characteristic diameter was only slightly smaller; however, the spread parameter, n, was found to be much broader after the addition of fines (2.18 compared to 2.68 for the coarse bed material) as illustrated in Table 4.

The test matrix and primary response are presented in Table 5 sorted by U_g and then U_{move} so that test points are listed in paired duplicates. The tests were conducted in the sequence of the test ID numbers.

Table 5. 3^2 Fully Duplicated Randomized Factorial Design Including Both Coded and Actual Independent Parameters as Well as Primary Dependent Performance Parameters

		independent param						dependent param		
		coded			actual					
std no.	test ID	Fines	F_m	U_g	Fines (%)	U_{move} (cm/s)	U_g (m/s)	ΔP_r (kPa)	$M_{s,Spiral}$ (kg/s)	H_{sp} (m)
1	f2	−1	−1	−1	0	3.0	5.3	6.03	2.81	8.4
9	f6	−1	−1	−1	0	3.0	5.3	6.23	2.81	8.2
2	f26	1	−1	−1	19	3.0	5.3	7.85	3.63	8.2
10	f18	1	−1	−1	19	3.0	5.3	7.76	3.59	8.4
11	f5	−1	1	−1	0	4.7	5.3	11.43	3.75	7.3
3	f4	−1	1	−1	0	4.7	5.3	11.28	3.84	7.2
4	f22	1	1	−1	19	4.7	5.3	13.84	5.00	7.1
12	f23	1	1	−1	19	4.7	5.4	13.79	5.12	7.1
5	f1	−1	−1	1	0	3.0	6.9	4.48	3.02	8.7
13	f3	−1	−1	1	0	3.0	6.8	4.44	2.93	8.7
14	f24	1	−1	1	19	3.0	6.9	6.13	3.72	8.6
6	f21	1	−1	1	19	3.0	6.9	5.95	3.64	8.7
15	f8	−1	1	1	0	4.8	6.9	7.51	4.24	7.8
7	f7	−1	1	1	0	4.8	6.8	7.60	4.11	7.8
8	f25	1	1	1	19	4.7	6.9	9.52	5.43	8.6
16	f20	1	1	1	19	4.7	6.9	9.51	5.26	8.0

Table 6. ANOVA for ΔP_r Computed Using $\alpha = 0.05$ and Exhibiting Adjusted $R^2 = 0.995$'

source	type I sum of squares	df	mean square	F	sig
corrected model	2.788	4	0.697	692.32	0.0000
intercept	23.363	1	23.363	23204	0.0000
U_g	0.699	1	0.699	694.15	0.0000
U_{move}	1.665	1	1.665	1654.1	0.0000
Fines	0.310	1	0.310	307.59	0.0000
U_gU_{move}	0.114	1	0.114	113.47	0.0000
error	0.011	11	0.001		
total	26.162	16			
corrected total	2.799	15			

Inspection of the duplicate pairs of data provides a sense of the reproducibility.

The analysis of variance (ANOVA) was conducted to evaluate the significance of the independent variables. Because the tests were conducted with fines as a blocked variable, the interactions between operating parameters and fines could not be evaluated. The GLM tested included the following factors: U_g, U_{move}, Fines, and the product of U_gU_{move}. The results of the ANOVA are presented in Tables 6−8 for ΔP_r, G_s, and H_{sp}, respectively. The ANOVA evaluates the contributions from each factor in the model, the intercept, and the error. Each factor is compared against the error to assess whether the factor is statistically different, using the F test at 95% confidence level as the criteria to determine significance. In these analyses any interactions between the fines level and the riser or standpipe air flows were assigned to the error. This provided a realistic, albeit conservative, estimate of the error.

The solids holdup in the riser, as indicated by ΔP_r, was dependent upon all three independent variables as well as the interaction (Table 6). In other words, the factors U_g, U_{move}, Fines, and U_gU_{move} all significantly influence ΔP_r. The effect of each of these variables on ΔP_r is presented in Figure 4. In this figure the dependent parameter used was the actual Sauter mean diameter measured during each test condition rather than the two levels used in the model. Contrary to laboratory tests in the FFB regime,[26−28] the smaller size bed material, with added fines, produced higher ΔP_r. The

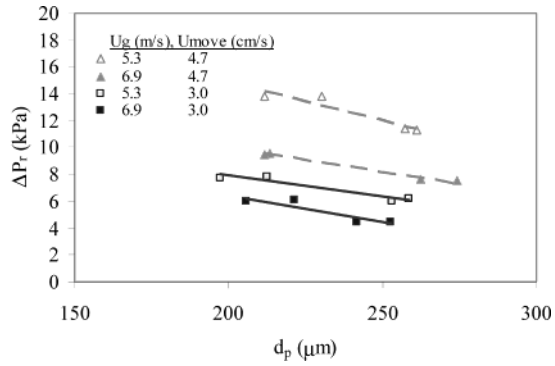

Figure 4. Dependence of ΔP_r on Fines, U_g, and U_{move}.

explanation for this discrepancy is in the different selection of independent factors. The laboratory tests operated with a fixed circulation rate; this study was operated much like an industrial facility with constant standpipe aeration, resulting in an increase in the circulation rate upon adding fines to the recycle. Our result was consistent with the enhanced performance in an industrial facility upon improvement of the cyclone efficiency.[29]

The effects of the gas velocity and standpipe aeration are also presented in Figure 4. Inspection of this figure reveals that, as expected based on the literature, an increased gas velocity resulted in a decreased ΔP_r.[17,18,27,28,33] The effect of increased standpipe aeration is primarily to move more solids into the riser, i.e., increase the circulation rate. As expected, an increased U_{move} resulted in an increased ΔP_r.

The nature of the significance of an interaction between U_g and U_{move} was a result of the tests being conducted near the FFB regime. The standpipe aeration, U_{move}, had a larger impact on moving more solids into the riser when the riser velocity, U_g, was lower. The riser held more solids at the lower velocity, and this tendency increased even more at the higher circulation rate. The voidage in the riser decreased from 98% at the higher velocity (Figure 5c,d) to about 97% at the lower velocity (Figure 5b), and this decreased further to about 95% at the higher circulation rate (Figure 5a). This is near the transition from dilute transport into fast fluidization as identified theoretically by Matsen[37] and observed experimentally.[38] The transition with increased fines was sufficient to increase the solids loading in the riser, resulting in an increased ΔP_r. At higher U_g, the riser held fewer solids, and an increase in U_{move} resulted in less of an impact upon ΔP_r.

Table 7. ANOVA for M_s Computed Using $\alpha = 0.05$ and Exhibiting Adjusted $R^2 = 0.967$

source	type I sum of squares	df	mean square	F	sig
corrected model	699 807 926	4	1.75×10^8	112.2	0
intercept	1.5501×10^{10}	1	1.55×10^{10}	9941	0
U_g	12 570 570.3	1	12 570 570	8.062	0.016
U_{move}	441 378 081	1	4.41×10^8	283.06	0
Fines	243 063 690	1	2.43×10^8	155.88	0
U_gU_{move}	2 795 584	1	2 795 584	1.793	0.208
error	17 152 130.3	11	1 559 285		
total	1.6218×10^{10}	16			
corrected total	716 960 056	15			

The mass circulation rate, M_s, was dependent upon each of the main factors, i.e., U_g, U_{move}, and Fines (Table 7). The F test indicated that each of these factors was significant at the 95% confidence level. As expected, M_s increased strongly with an increase in U_{move}. A higher U_g induced a small but significantly higher M_s, but an increased Fines level resulted in a remarkably large increase in M_s (Figure 6). As found in Table 1, the fines concentration increased the bulk density of the bed; however, the bed density in the standpipe is somewhat less than that of the packed bed[36] though, as yet, unpredictably so. Thus, the circulation rates as determined by the spiral were calculated assuming the same bed density, making the reported M_s with added fines conservatively low. On the basis of the findings of the fines effect in fluidized beds,[10−14] transport lines,[15,16] and nonmechanical valves,[31,32] the increase in the solids flux with the added fines can be thought to be a result of the solids filling the void in the packed bed of solids moving down the standpipe, reducing the permeability, increasing the U_{move} split of aeration toward the riser, and increasing the velocity and momentum, thereby dragging more solids into the riser.

The observed steady-state height of solids in the standpipe, H_{sp}, was dependent upon the operating

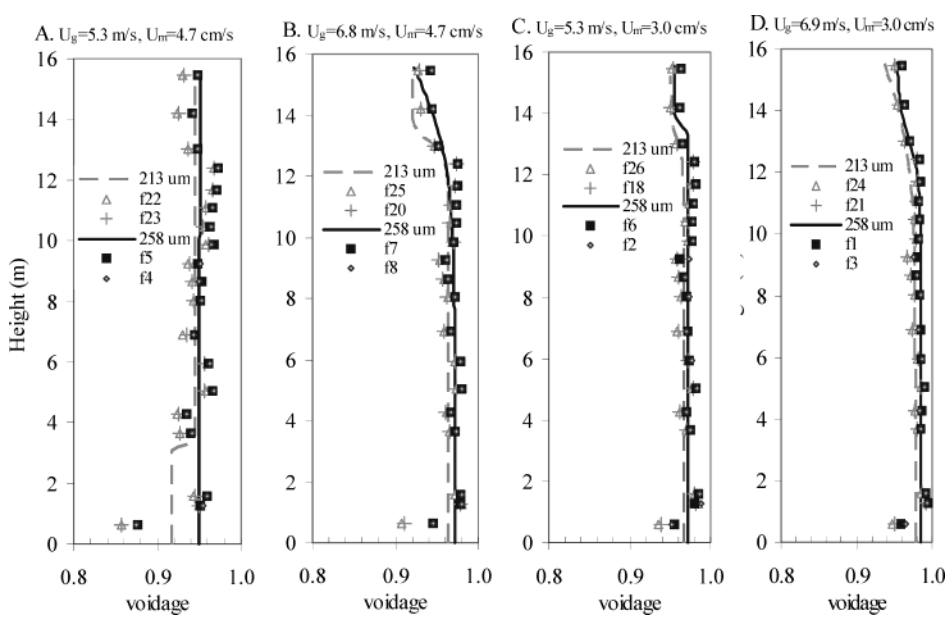

Figure 5. Axial riser voidage profile comparing the initial coke with a coke + fines mixture under identical aeration conditions.

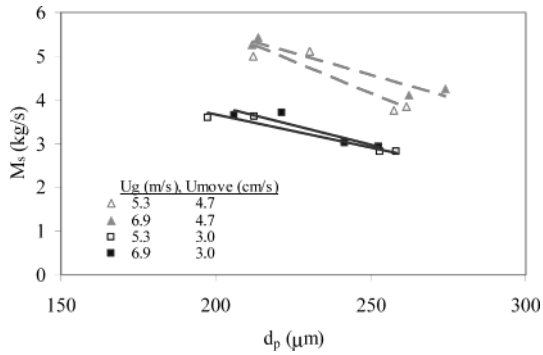

Figure 6. Dependence of M_s on Fines, U_g, and U_{move}.

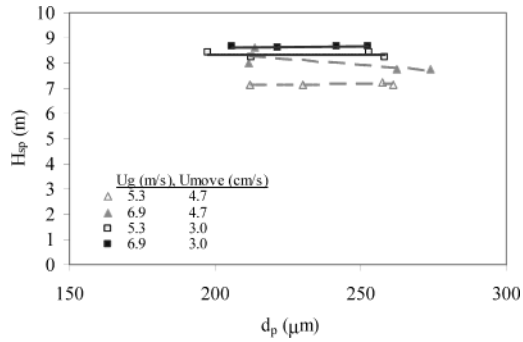

Figure 7. Dependence of H_{sp} on Fines, U_g, and U_{move}.

Table 8. ANOVA for H_{sp} Computed Using $\alpha = 0.05$ and Exhibiting Adjusted $R^2 = 0.880$'

source	type I sum of squares	df	mean square	F	sig
corrected model	52.487	4	13.122	28.403	0
intercept	11 146.081	1	11146.08	24126	0
U_g	15.016	1	15.016	32.502	0
U_{move}	33.931	1	33.931	73.445	0
Fines	0.391	1	0.391	0.846	0.378
U_gU_{move}	3.151	1	3.151	6.82	0.024
error	5.082	11	0.462		
total	11 203.65	16			
corrected total	57.569	15			

conditions (U_g, U_{move}, and U_gU_{move}) but independent of Fines (Table 8). The horizontal lines in the plot of H_{sp} versus d_p in Figure 7 demonstrate this lack of influence that fines had on H_{sp}. This lack of dependence on fines is consistent with the test designed with a constant total inventory in the CFB loop. The response of H_{sp} to process operating conditions was inversely related to the response of the apparent solids holdup in the riser, ΔP_r. This provided corroboration of the interpretation that ΔP_r was a measure of the mass of the solids in the riser.

The axial voidage profile along the riser was analyzed for each operating condition (Figure 5a−d). In this figure, the tests with fines are represented by solid lines and symbols while the coarse bed materials are dotted lines. The reproducibility was excellent. The operating conditions generated relatively uniform axial profiles with only minimal inlet and end effects and only a small hint of a dense bed at the base of the riser for the test case with the lowest riser flow and highest standpipe aeration (Figure 5a). The most notable observation from these profiles was the fact that the added fines produced lower voidage consistently up and down the riser in all conditions. This is consistent with the result that fines increased the solids circulation rate and the solids holdup in the riser.

Conclusion

A series of tests were conducted using randomized duplicated factorial design. Unbiased measurement of error was estimated in order to establish the significance of several response variables to the independent factors. A high degree of repeatability established that the presence of fines increased ΔP_r and M_s but not H_{sp}. These findings provide one factor explaining the improved process performance reported for industrial units after increasing the cyclone efficiency.[29,39] Solids circulation is the primary operating parameter influencing the overall CFB performance in the area of gas−solids mixing. Increases in the circulation of solids and solids loading in the riser improve mixing, heat transfer, and moderate temperature. The presence of fines significantly and drastically affects the solids flux and solids holdup in the riser even in the more dilute regions of the bed.

Acknowledgment

The authors acknowledge the Department of Energy for funding the research through the Fossil Energy's Combustion Systems and Advanced Research for Power Programs. Operations of the CFB unit were made possible with support from Larry Lawson, Jim DeVault, Dave Lunifeld, and Todd Worstell.

Symbols

A = cross-sectional area (m^2)
A_r = riser cross-sectional area (m^2)
d = sieve size (μm)
d_c = characteristic diameter in the Rosin−Rammler distribution (μm)
D_{riser} = riser diameter (m)
D_{sp} = standpipe diameter (m)
f = functional relationship for a desired variable
E_{rss} = root mean sum of squares error
F_{431} = transport gas flow through riser flow controller (m^3/h)
F_{421} = transport gas flow through riser flow controller (m^3/h)
F_{372} = fluidizing gas flow through loopseal flow controller (m^3/h)
g_c = gravitational constant (9.81 m/s^2)
GLM = general linear model
G_s = solids flux ($kg/m^2 \cdot s$)
H_{sp} = standpipe bed height (m)
I = coded level in the GLM
n = characteristic size distribution or spread in the Rosin−Rammler distribution
P_{act} = actual pressure (kPa)
P_{atmos} = atmospheric pressure (kPa)
P_{std} = standard pressure (kPa)
$P_{r,base}$ = pressure at the base of the riser (kPa)
PSD = particle size distribution
Q_s = solids volumetric flow (m^3/s)
t = time (s)
T_{act} = actual temperature (K)
T_r = riser temperature (K)
T_{std} = standard temperature (K)
u_i = variable, i, in the propagation of errors
U_g = superficial gas velocity (m/s)
U_{mf} = minimum fluidization velocity (m/s)
U_{move} = aeration at the base of the standpipe (m/s)
U_t = terminal velocity (m/s)
V = volume (m^3)
X = independent parameters

Y = cumulative percent solids in sieve analysis (wt %)

Greek Letters

α = average coefficients in the GLM
β = differential coefficients in the GLM
ϵ = voidage
ϵ_b = bed voidage
ϵ_{mf} = minimum fluidization voidage
ρ_b = bed density (kg/m^3)
ρ_s = solid density (kg/m^3)
ϕ = sphericity
σ_s = PSD as 1 standard deviation from the Sauter mean (μm)
Δ = difference between two states
ΔL = increment length (m)
ΔP = pressure drop (kPa)
ΔP_r = pressure drop across the entire length of the riser (kPa)

Literature Cited

(1) Robertson, A.; Domeracki, W.; Newby, R.; Rehmat, A.; Horazak, D. *Second-generation pressurized fluidized bed combustion plant—conceptual design and optimization of a second generation PFB combustion plant*; FWDC Phase 2 Annual Report (Oct 1, 1991−Sept 30, 1992, FWC/FWDC-TR-92/11 DE-AC21-86MC21023).

(2) Froehlich, R.; Robertson, A.; VanHook, J.; Goyal, A.; Rehmat, A.; Newby, R. *Second-generation pressurized fluidized bed combustion plant research and development Phase 2−Task 4 Carbonizer testing*; DE-AC21-86MC21023; 1994; p 267.

(3) Smith, P. V.; Vimalchand, P.; Pinkston, T.; Henningsen, G.; Longanbach, J. Transport Reactor Combustor and Gasifier Operations. *Energex 2000: Proceedings of the 8th International Energy Forum*, Las Vegas, NV, Jul 23−28, 2000; p 94.

(4) Davis, B. M.; Vimalchand, P.; Liu, G.; Smith, P. V.; Longanbach, J. Operation of the PSDF Transport Gasifier. *Nineteenth Annual Pittsburgh Coal Conference*, Pittsburgh, PA, Sept 23−27, 2002; p 16; Paper 1728.

(5) Bissett, L. A. Hot/warm gas cleanup. *Proceedings of the Vision 21 Program Review Meeting*, Morgantown, WV, Nov 6 and 7, 2001; p 6; DOE/NEIL-2002/1168 (CD-ROM).

(6) Turton, R.; Berry, D. A.; Gardner, T. H.; Miltz, A. The evaluation of zinc oxide sorbents in a pilot transport reactor: sulfidation kinetics and reactor modeling. *Ind. Eng. Chem. Res.* **2004**, *43* (5), 1235−1243.

(7) Gauthier, D.; Zerguerras, S.; Flamant, G. *Chem. Eng. J.* **1999**, *74*, 181−196.

(8) Lin, C.-L.; Wey, M.-Y.; You, S.-D. The effect of particle size distribution on minimum fluidization velocity at high temperature. *Powder Technol.* **2002**, *126*, 297−301.

(9) Ray, Y. C.; Jiang, T. S.; Wen, C. Y. *Powder Technol.* **1987**, *49*, 193−206.

(10) Cheung, L.; Nienow, A. W.; Rowe, P. N. *Chem. Eng. Sci.* **1974**, *29*, 1301−1303.

(11) Geldart, D.; Cullinan, J.; Georghiades, D.; Gilvray, D.; Pope, D. J. *Trans. Inst. Chem. Eng.* **1979**, *57*, 269.

(12) Geldart, D.; Pope, D. J. *Powder Technol.* **1983**, *34*, 95.

(13) Kwauk, M. *Fluidization*; Science Press: New York, 1992; p 39.

(14) Choi, J.-H.; Suh, J.-M.; Chang, I.-Y.; Shun, D.-W.; Yi, C.-K.; Son, J.-E.; Kim, S.-D. The effect of fine particles on elutriation of coarse particles in a gas fluidized bed. *Powder Technol.* **2001**, *121*, 190−194.

(15) Hyder, L. M.; Bradley, M. S. A.; Reed, A. R.; Hettiaratchi, K. An investigation into the effect of particle size on straight-pipe pressure gradients in lean-phase conveying. *Powder Technol.* **2000**, *112*, 235−243.

(16) Hayden, K. S.; Park, K.; Curtis, J. S. Effect of particle characteristics on particle pickup velocity. *Powder Technol.* **2003**, *131*, 7−14.

(17) Li, Y.; Kwauk, M. In *Fluidization*; Grace, J. R.; Matsen, J. M., Eds.; Plenum: New York, 1980; p 537.

(18) Yerushalmi, J.; Cankurt, N. T. Further studies of the regimes of fluidization. *Powder Technol.* **1979**, *24*, 187−205.

(19) Brereton, C.; Stromberg, L. In *Circulating Fluidized Bed Technology*; Basu, P., Ed.; Pergamon: New York, 1986; pp 133−144.

(20) Shnitzlein, M.; Weinstein, H. In *Circulating Fluidized Bed Technology II*; Basu, P., Large, J. F., Eds.; Pergamon: New York, 1988; p 205.

(21) Jin, Y.; et al. In *Fluidization '88—Science and Technology*; Kwauk, M., Kunii, D., Eds.; Science Press: Beijing, 1988; p 165.

(22) Arena, U.; et al. In *Circulating Fluidized Bed Technology II*; Basu, P., Large, J. F., Eds.; Pergamon: New York, 1988; p 265.

(23) Hartge, E. U.; Li, Y.; Werther, J. In *Fluidization V*; Ostergaard, K., Sorensen, A., Eds.; Engineering Foundation: New York, 1986; p 345.

(24) Jiang, P. J.; et al. In *Proceedings of the International Symposium on Multiphase Flows*; Fan, Z. Q., Crowe, C. T., Eds.; Hangzhoy: China, 1987; Vol. 1, p 94.

(25) Arena, U.; Massimilla, L.; Pirozzi, D. FBC Comes of Age. In *Proceedings of the 1987 International Conference on Fluidized Bed Combustion*; Mustonen, J. P., Ed.; The American Society of Mechanical Engineers: New York, 1987; Vol. 2, p 762.

(26) Sun, G.; Grace, J. R. Effect of particle Size Distribution in Different Fluidization Regimes. *AIChE J.* **1992**, *38*, 716−722.

(27) Bai, D.-R.; Jin, Y.; Yu, Z.-Q.; Zhu, J.-X. The axial distribution of the cross-sectionally averaged voidage in fast fluidized beds. *Powder Technol.* **1992**, *71*, 51−58.

(28) Adanez, J.; Gayan, P.; Garcia-Labiano, F.; de Diego, L. F. Axial voidage profiles in fast fluidized beds. *Powder Technol.* **1994**, *81*, 259−268.

(29) Lee, J.-M.; Kim, J.-S.; Kim, J.-J. Evaluation of the 200 MWe Tonghae CFB boiler performance with cyclone modification. *Energy* **2003**, *28*, 575−589.

(30) Kim, S. W.; Kim, S. D. Effects of particle properties on solids recycle in loop-seal of a circulating fluidized bed. *Powder Technol.* **2002**, *124*, 76−84.

(31) Kim, S. W.; Namkung, W.; Kim, S. D. Solids flow characteristics in loop-seal of a circulating fluidized bed. *Korean J. Chem. Eng.* **1999**, *16*, 82−88.

(32) Knowlton, T. M. In *Circulating Fluidized Bed Technology II*; Basu, P., Large, J. F., Eds.; Pergamon: New York, 1988; pp 31−41.

(33) Smolders, K.; Baeyens, J. Gas fluidized beds operating at high velocities: a critical review of occurring regimes. *Powder Technol.* **2001**, *119*, 269−291.

(34) Ludlow, J. C.; Shadle, L. J.; Syamlal, M. Method to continuously monitor Solids Circulation Rate. In *Circulating Fluidized Bed Technology VII*; Grace, J. R., Zhu, J., de Lasa, H., Eds.; Canadian Society of Chemical Engineering: Ottawa, Canada, 2002; pp 513−520.

(35) Doebelin, E. O. *Measurement Systems Application and Design*, 3rd ed.; McGraw-Hill Book Co.: New York, 1983.

(36) Monazam, E. R.; Shadle, L. J.; Ludlow, J. C.; Ontko, J. Improvement of Continuous Solid Circulation Rate Measurement in Cold Flow Circulating Fluidized Bed. *Powder Technol.* **2004**, submitted for publication.

(37) Matsen, J. M. Mechanisms of Choking and Entrainment. *Powder Technol.* **1982**, *32*, 21−33.

(38) Shadle, L. J.; Monazam, E. R.; Mei, J. S. Characterization of Operating Flow Regimes in a Cold Flow Circulating Fluid Bed. In *Circulating Fluidized Bed Technology VII*; Grace, J. R., Zhu, J., de Lasa, H., Eds.; Canadian Society of Chemical Engineering: Ottawa, Canada, 2002; pp 255−262.

(39) Ogunsola, O. I.; Shadle, L.; Casleton, K.; Mei, J. Investigation of the Causes of Seasonal Variation of NOx Emission from Waste Coal-Fired Circulating Fluidized Bed Utility Plant. *Ind. Eng. Chem. Res.* **2001**, *40* (18), 3869−3878.